Am J Cancer Res 2017;7(1):64-76
www.ajcr.us /ISSN:2156-6976/ajcr0045230

Original Article

The malignancy of miR-18a in human glioblastoma via directly targeting CBX7

Weining Wu*, Xu Zhou*, Tianfu Yu, Zhongyuan Bao, Tongle Zhi, Kuan Jiang, Er Nie, Yingyi Wang, Junxia Zhang, Yongping You

*Department of Neurosurgery, The First Affiliated Hospital of Nanjing Medical University, Nanjing 210000, Jiangsu, China. *Equal contributors.*

Received November 27, 2016; Accepted December 15, 2016; Epub January 1, 2017; Published January 15, 2017

Abstract: Aberrant levels of microRNAs (miRNAs) are linked to tumorigenesis and tumor progression. Here we analyzed the expression of microRNA 18a in glioblastoma multiforme (GBM) within groups of coexpressed groups of genes through analysis of expression profiling databases and clinical tissues. Cell proliferation and flow cytometry experiments were performed to determine the roles of miR-18a in the proliferation of glioblastoma cells in vitro. We employed bioinformatics analyses, luciferase reporter assays, and immunoblotting to identify chromobox protein homolog 7 (CBX7) as the target gene of miR-18a. A significant inverse correlation was observed between miR-18a and CBX7 expression in GBM tissues ($r = -0.6264$, $P = 0.0094$). Bioinformatics analyses revealed that most CBX7-associated genes were enriched in terms associated with cell cycle pathways. Upregulated expression of CBX7 inhibited the growth of GBM cells and reduced the expression of CDK2 and cyclin A2 (CCNA2). Rescue experiments indicated that overexpression of CBX7 significantly recovered the increase in cell proliferation and cell cycle distribution induced by miR-18a overexpression. In vivo studies revealed that decreased levels of miR-18a delayed the growth of intracranial tumors, which was accompanied by increased CBX7 expression. We suggest that miR-18a promotes glioblastoma progression via altering CBX7 expression and therefore may serve as a potential target for treating glioblastoma.

Keywords: Glioblastoma, proliferation, microRNA, target genes, tumorigenesis

Introduction

Glioblastoma multiforme (GBM) is the most common histological subtype of this lethal primary brain tumor in adults [1]. Despite advances in standard therapy over the past several decades, such as surgery, radiation, and chemotherapy, the prognosis of patients with GBM remains poor, with a median survival time ranging from 9 to 12 months [2]. Thus, further studies are required to develop new molecular targets and treatment strategies for this disease.

MicroRNAs (miRNAs) are noncoding RNAs that regulate diverse biologic processes by binding to a complementary sequence in the 3'-UTR of target mRNAs, which inhibits translation [3]. MiRNAs are involved in human tumorigenesis by regulating the expression of oncogenes and tumor suppressor genes. For example, the members of the classic let-7 family of tumor suppressors inhibit tumorigenesis, cancer cell proliferation, metastasis, and induce apoptosis [4, 5]. MiR-21 was the first miRNA detected in the human genome, and it enhances the oncogenic phenotype by targeting tumor suppressor genes [6, 7]. Our previous study of gliomas revealed that miR-675 expression correlates with the World Health Organization's grading of gliomas and promotes glioma invasion by targeting *CDH13* mRNA [8]. However, there are still grade-associated miRNAs in gliomas need further researches about influencing glioma phenotypes.

Chromobox protein homolog 7 (CBX7), one of five mammalian orthologs of *Drosophila* polycomb, is a member of the polycomb repressive complex 1 (PRC1), which maintains developmental regulatory genes in a silenced state [9, 10]. CBX7 maintains the balance between self-renewal and differentiation in embryonic stem cells (ESCs) and hematopoietic stem cells (HSCs) [11, 12]. In tumors, although a low level

of CBX7 is associated with a more aggressive phenotype of breast, bladder, pancreatic, and colon carcinomas [13-16], the mechanism of tumor suppression is unclear. Recently, an article brings inspiration that CBX7 modulates cyclin E (CCNE1) expression through binding to histone deacetylase 2 (HDAC2), which mediates its activities specific for the *CCNE1* promoter [17]. Also the research on inhibited role of CBX7 in migration of glioblastoma have been reported [18].

Here we show that the expression of oncogenic miR-18a correlated with WHO grade and was upregulated in clinical GBM samples. Moreover, we identified *CBX7* mRNA as a direct target of miR-18a, which was down-regulated in GBM tissues, and that the levels miR-18a inversely correlated with those of CBX7. Gene-enrichment analysis revealed that CBX7-associated genes from three independent GBM databases were significantly enriched in cell cycle components. Further, miR-18a controlled the proliferation of GBM cells and regulated the cell cycle through abrogating the inhibition by CBX7 of the expression of cell cycle-related genes. Our data indicate that miR-18a may serve as a critical therapeutic target for GBM intervention strategies.

Materials and methods

Glioblastoma cell lines and primary GBM cell lines

The human glioma cell lines U87, U251, Ln229, T98, U118, and H4 were purchased from the Chinese Academy of Sciences Cell Bank (Shanghai, China). A primary culture designated GBM1 was established in February 2016 from the tumor cells of a patient with a left frontal glioblastoma, and a culture designated GBM2 was established in March 2016 from tumor cells taken from a patient with a left tempus glioblastoma. Tumor tissue was collected from a patient who granted written informed consent. The Institutional Review Board of the First Affiliated Hospital of Nanjing Medical University approved the study protocol.

Tissue was obtained from regions comprising viable tumor cells. Within 2 h after acquisition, the tissue samples were dissociated into single-cell suspensions, washed with Hanks solution (Solarbio, Beijing, China) to remove red blood cells, and the number of cells was counted. The primary cultures were maintained in serum. All GBM cell lines were preserved in liquid nitrogen. All cell lines were cultured in Dulbecco's modified Eagle's medium (DMEM) (Hyclone Laboratories, Utah, USA) supplemented with 10% fetal bovine serum (FBS) (Gibco, CA, USA) at 37°C in an atmosphere containing 5% CO_2.

Human brain tissues and study approval

Glioblastoma specimens (n = 16) and adjacent normal brain tissue (NBT) (n = 16) were obtained from The First Affiliated Hospital of Nanjing Medical University. The Research Ethics Committee of Nanjing Medical University (Nanjing, Jiangsu, China) approved the use of GBMs and adjacent normal tissues, and the procedures were performed in accordance with the approved guidelines. The express permissions from participants were obtained, and patients granted informed consent.

Three gene expression profiling cohorts of gliomas were used in this study. The miRNA expression microarray data for 158 gliomas were downloaded from the Chinese Glioma Genome Atlas (CGGA) data portal (http://www.cgga.org.cn/portal.php). The samples included 48 astrocytomas (A, WHO Grade II), 13 oligodendrogliomas (O, WHO Grade II), 8 anaplastic astrocytomas (AA, WHO Grade III), 10 anaplastic oligodendrogliomas (AO, WHO Grade III), 15 anaplastic oligoastrocytomas (AOA, WHO Grade III), and 64 GBMs (WHO Grade IV). The mRNA expression microarray data for 216 gliomas were downloaded from the CGGA, which included 58 A, 18 O, 21 oligoastrocytomas (OA, WHO Grade II), 8 AA, 11 AO, 15 AOA, 85 GBM. Gene expression data (226 WHO II, 249 WHO III, 403 GBM) were downloaded from The Cancer Genome Atlas (TCGA) database (http://tcgadata.nci.nih.gov/). Gene expression profiling data for 153 glioma samples were collected from GSE4290 (https://www.ncbi.nlm.nih.gov/geo/query/acc.cgi?acc = GSE4290), including 45 WHO II, 31 WHO III, 77 GBM.

Hsa-miR-18a mimic, inhibitor, plasmid construction, and transfection

An Hsa-miR-18a mimic, an Hsa-miR-18a inhibitor, and an hsa-miR-scramble, were chemically synthesized by Ribobio (Guangzhou, China). A plasmid containing the human *CBX7* coding sequence was constructed according to the manufacturer's protocol (Genechem; Shanghai,

China). A human *CBX7* cDNA was inserted into the vector pGL3 to generate pGL3-CBX7. All oligonucleotides and plasmids were transfected using Lipofectamine 2000 Transfection Reagent (Invitrogen, CA, USA) according to the manufacturer's instructions.

Lentiviral packaging and establishment of stably transduced cell lines

A lentiviral packaging kit was purchased from Genechem (Shanghai, China). A lentivirus carrying hsa-miR18a-down or hsa-miR-negative control (miR-NC) was packaged in the human embryonic kidney cell line 293T, and the virions were collected according to the instructions in the manufacturer's manual. Stable cell lines were established by infecting U87 cells with lentiviruses, followed by puromycin selection.

RNA isolation and quantitative real-time PCR (qPCR)

RNA was extracted from cell lines and fresh tissues using TRIzol reagent (Life Technologies, CA, USA) following the manufacturer's protocol. Quantitative real-time PCR was conducted using the ABI StepOne Plus system (Applied Biosystems, CA, USA) with the Bulge-loop miRNAqRT-PCR Primer Kit (Ribobio, Guangzhou, China) to detect miR-18a-5p. Primers were purchased from Ribobio. Data were analyzed using the $2^{-\Delta\Delta Ct}$ method, and U6 RNA was used as endogenous control.

Protein extraction and immunoblotting

Protein extraction and immunoblotting were performed as described previously [19]. Briefly, cells or tissues were lysed on ice for 30 min in radioimmunoprecipitation assay buffer. The lysates were centrifuged at 12,000 rpm at 4°C for 15 min, the supernatants were collected, and protein concentrations were determined using the bicinchoninic acid assay (KenGEN, Jiangsu, China). Equal amounts of protein were separated using 10% SDS-PAGE followed by electrotransfer of the proteins onto a polyvinylidene difluoride membrane (Thermo Fisher Scientific, MA, USA). Membranes were blocked with 5% nonfat milk for 2 h and incubated with primary antibodies. An electrochemiluminescence detection system (Thermo Fisher Scientific) was used for signal detection. Antibodies against CBX7, Cyclin A2, CDK2, and β-actin were obtained from Cell Signaling Technology (MA, USA).

Cell proliferation assay

Exponentially growing cells were seeded at 3,000 cells per well and cultured in 96-well plates. Cell proliferation was assayed using the Cell-Counting Kit 8 (CCK8, Dojindo Laboratories, Japan) at the indicated times according to the manufacturer's instructions. A colony formation assay was performed as described previously [20]. Briefly, 1×10^2 cells were independently plated onto 6-well tissue culture plates. After 10-20 days, visible colonies were fixed with 4% paraformaldehyde for 20 min and stained with 0.1% crystal violet for 12 h. Colony-forming efficiency was calculated as the number of colonies (diameter > 0.5 mm). The Molecular Probes EdU-Alexa imaging detection kit was purchased from Life Technologies (MA, USA). Cells transfected 48 h earlier were incubated with 10 μM EdU for 2 h, fixed, permeabilized, and stained with the Alexa-Fluor 594 reaction cocktail for EdU and Hoechst 33342 for cell nuclei, following by the manufacturer's protocol. Samples were imaged using a fluorescence microscope. All assays were repeated at least three times.

Flow cytometric analysis of the cell cycle

Transfected cells were harvested, washed with phosphate-buffered saline (PBS), fixed with 70% ice-cold ethanol, resuspended using a Cell Cycle Staining Kit (Multi Sciences, Hangzhou, China), and incubated for 30 min in the dark before being analyzed using flow cytometry.

Dual luciferase reporter assay

The wild-type (WT) and mutated (Mut) putative miR-18a seed matching sites of the CBX7 3'-untranslated regions (UTRs) were amplified using PCR from human cDNA, inserted into the Sac I and Hind III sites, and cloned into the pmiRNA-Report vector (Genechem, Shanghai, China). U87 and PG1 cells were seeded in a 24-well plate and cotransfected with the WT or Mut reporter plasmid, a *Renilla* luciferase (pRL) plasmid, and the miR-18a mimic or miR-scramble. Luciferase activities were analyzed 24 h after transfection using the Promega Dual Luciferase Reporter Assay System (WI, USA).

Nude mouse model of intracranial glioma

Animal experiments were approved by the Animal Management Rule of the Chinese Ministry of Health (document 55, 2001) and were in

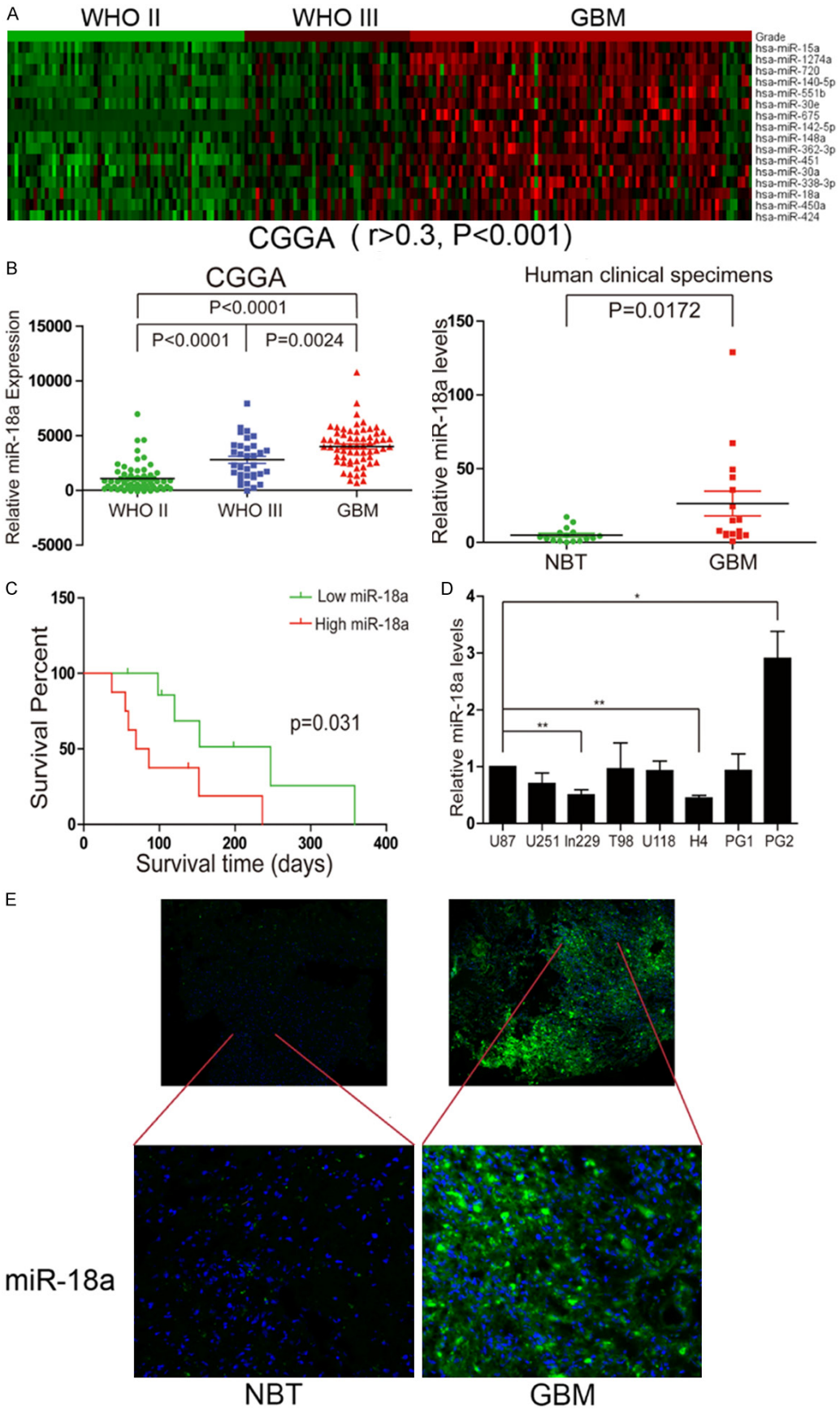
A
WHO II
WHO III
GBM
Grade
hsa-miR-15a
hsa-miR-1274a
hsa-miR-720
hsa-miR-140-5p
hsa-miR-551b
hsa-miR-30e
hsa-miR-675
hsa-miR-142-5p
hsa-miR-148a
hsa-miR-362-3p
hsa-miR-451
hsa-miR-30a
hsa-miR-338-3p
hsa-miR-18a
hsa-miR-450a
hsa-miR-424
CGGA (r>0.3, P<0.001)
B
CGGA
P<0.0001
P<0.0001
P=0.0024
Relative miR-18a Expression
15000
10000
5000
0
-5000
WHO II
WHO III
GBM
Human clinical specimens
P=0.0172
Relative miR-18a levels
150
100
50
0
NBT
GBM
C
Low miR-18a
High miR-18a
Survival Percent
150
100
50
0
p=0.031
0
100
200
300
400
Survival time (days)
D
Relative miR-18a levels
4
3
2
1
0
*
**
**
U87
U251
In229
T98
U118
H4
PG1
PG2
E
miR-18a
NBT
GBM

Figure 1. MiR-18a expression correlates positively with malignant degrees of glioma. A. Heat map showing significantly positively-expressed miRNAs with WHO grade in CGGA Public database ($r > 0.3$, $P < 0.01$). B. Expression of miR-18a positively correlates with WHO grade in CGGA Public database, and relative levels of miR-18a in the tumors and their adjacent normal brain tissues from 16 patients diagnosed as glioblastomas. C. Correlation between miR-18a expression and the overall survival of GBM patients by Kaplan-Meier survival curves. A log-rank test was used to assess the statistical significance of the differences. D. Relative expressions of miR-18a in glioma cell lines U87, U251, Ln229, T98, U118, H4, and primary glioma cells from two patients. E. The different expressions of miR-18a were determined by FISH in glioblastoma and adjacent normal tissue respectively from a typical patient. *$P < 0.05$, **$P < 0.01$.

conducted in accordance with the approved guidelines and experimental protocols of Nanjing Medical University. Twelve nude mice 3-4 weeks of age were purchased from the Shanghai Experimental Animal Center of the Chinese Academy of Sciences and randomly divided into two groups. Viable miR-18a-down and miR-NC-infected U87 cells (2.5×10^5) were intracranially injected into nude mice to generate intracranial gliomas. The mice were imaged for Fluc activity using a bioluminescence imaging system (Caliper IVIS Spectrum, USA) on days 7, 14, 21, and 28 after implantation. The Living Images software package (Caliper Life Sciences) was used to determine the integrated flux of photons (photons per second) within each region. The mice were killed at the end, and the brains were extracted and fixed in 10% formalin and then embedded in paraffin for hematoxylin and eosin staining and immunohistochemical anlaysis.

Immunohistochemistry (IHC)

IHC was used to analyze fresh brain tissues and intracranial tumor tissues of the nude mice to detect and evaluate CBX7 expression using methods described previously [21].

Fluorescence in situ hybridization (FISH)

The probes used for in situ hybridization to detect miR-18a were synthesized by GoodBio (Wuhan, China). Fresh tissues were fixed in 4% formaldehyde for 1 h and then dehydrated in 15% sucrose for 8 h. The tissues were fixed in 4% formaldehyde for 10 min, washed three times for 5 min each with PBS (pH 7.4), digested using proteinase K for 2 min, washed again three times for 5 min each using PBS (pH 7.4). After eliminating auto-fluorescence and blocking endogenous biotin, the sections were hybridized with the probes overnight. The tissue sections were then washed with warmed in 2 × SSC at 37°C for 10 min, 1 × SSC at 37°C for 10 min, and 0.5 × SSC for 10 min. After incubation in BSA for 30 min at room temperature, tissue sections were treated with Alexa Fluor 488-avidin (1:400), incubated at room temperature for 50 min, washed three times for 5 min each with PBS. Tissue sections were incubated with the primary antibody overnight and then with the species-specific secondary antibody for 50 min at 4°C. Finally, the tissue sections were washed twice with PBS and mounted using a medium containing DAPI.

Statistical analysis

All values are presented as the mean ± standard deviation (SD), and statistical analyses were performed using the Student *t* test to evaluate the significance of differences between groups, one-way ANOVA was used to determine the difference among at least three groups using SPSS v19.0 for Windows. (SPSS, IL, USA). Pearson's correlations analysis and heat map microarray analysis were implemented using Multiple Array Viewer 4.9 software (MEV). Kaplan-Meier survival analyses were done employing GraphPad 5.0 software. $P < 0.05$ indicates a significant difference.

Results

MiR-18a is upregulated in human glioma tissues

To investigate miRNA expression in human glioma tissues, comprehensive microarray analysis was performed to compare miRNA expression levels, including those of 158 glioma tissues. We queried the CGGA database to identify glioblastomas that expressed the detected miRNAs. Microarray analysis identified 16 significantly up-regulated miRNAs among 829 miRNAs that positively correlated with the patients' WHO Grades (Pearson's $r > 0.3$, $P < 0.01$) (**Figure 1A**). Among these miRNAs, we found that miR-18a was highly expressed in high-grade gliomas, especially in the glioblastomas included in the CGGA data (**Figure 1B**). MiR-18a expression levels were elevated in 16 human glioblastoma specimens compared with those

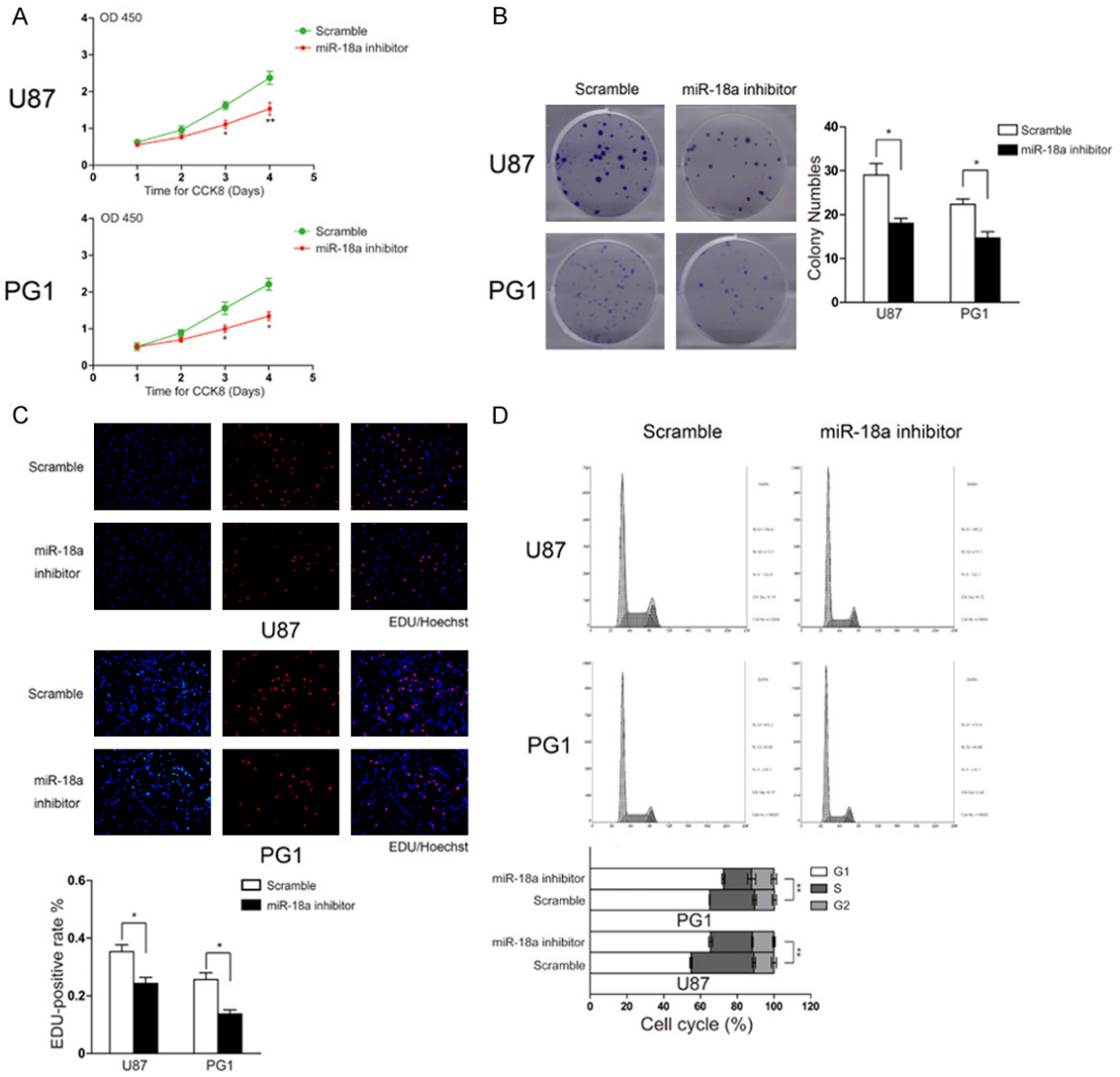

Figure 2. Decreasing miR-18a level inhibits cell proliferation and the cell cycle. A. Cell proliferation was detected by CCK8 assays in U87 and Primary glioblastoma cells transfected with scramble and miR-18a-5p inhibitor. B. Colony formation assays in U87 and Primary glioblastoma cells transfected with scramble and miR-18a-5p inhibitor. Scale bar > 500 μm. C. Respective merged images of U87 and Primary glioblastoma cells in EDU transfected with scramble and miR-18a-5p inhibitor after 48 h. Representative images were shown (original magnification, 200 ×). D. The cell cycle was detected in U87 and Primary glioblastoma cells transfected with scramble and miR-18a-5p inhibitor after 48 h. All experiments were performed 3 times, and average scores are indicated with error bars on the histogram. *P < 0.05, **P < 0.01.

of the adjacent normal brain tissues (**Figure 1B**). Kaplan-Meier survival analysis of these 16 patients revealed that high differential expression of miR-18a was associated with decreased survival compared with patients with miR-18a levels less than the median (P = 0.031) (**Figure 1C**). The relative levels of miR-18a in various glioma cells, including two types of primary GBM cells extracted acquired from two patients, were detected using q-PCR (**Figure 1D**). We chose one representative GBM specimen and the adjacent normal tissue for FISH analysis (**Figure 1E**).

MiR-18a enhances the malignant phenotpe of glioblastoma cells

To determine whether the abnormally high expression of miR-18a was associated with its biological role in gliomas, we performed a series of proliferative assays of the glioma cell line U87 and primary cells (PG1) obtained from

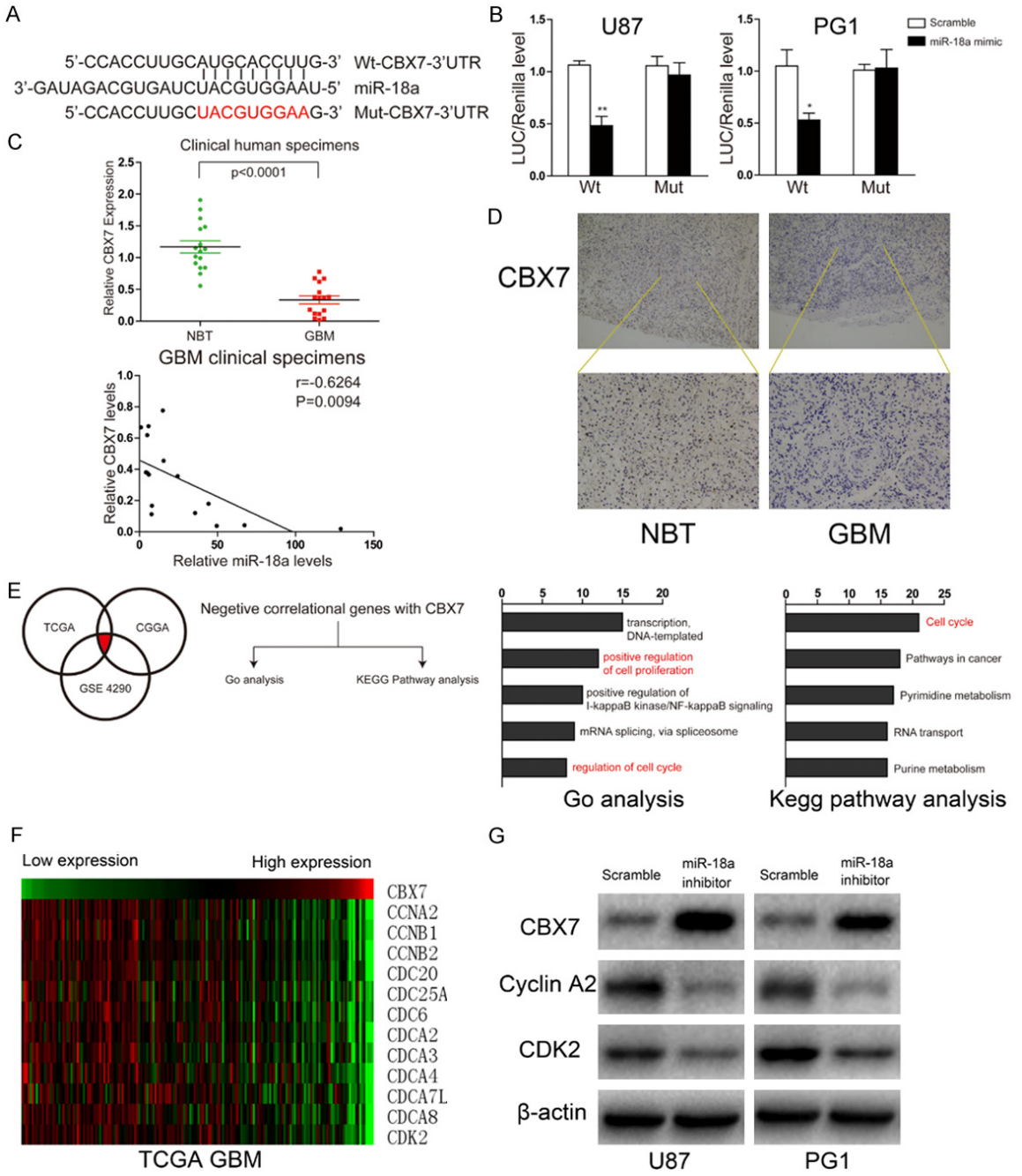

Figure 3. CBX7 is the direct target gene of miR-18a and negatively-associated genes of CBX7 were in positively-regulated cell cycle genes. A. Predicted miR-18a target sequence in the 3'UTR of CBX7 and mutant one containing altered nucleotides in the 3'UTR of CBX7. B. Luciferase assay of the indicated cells transfected with pmiRNA-Wt-CBX7-3'UTR, or pmiRNA-Mut-CBX7-3'UTR reporter with miR-18a mimic or miR-NC. **P < 0.01, *P < 0.05. C. The expression levels of CBX7 in 16 cases of glioblastoma specimens and adjacent normal brain tissues were determined by immunoblotting, the fold changes were normalized to β-actin. Pearson's correlation analysis was used to determine the correlations between the CBX7 protein expression and miR-18a levels in glioblastoma specimens. D. Immunohistochemistry analysis of CBX7 in two representative tissues (one GBM and one NBT specimens). E. CBX7 negatively-associated genes from Correlation analysis performed in the CGGA, TCGA, and GSE4290 glioblastoma samples were analyzed with gene ontology analysis and KEEG pathway analysis. Biological processes enrichment results from GO database and KEGG pathways analysis were shown. The orders of different biological processes were based on their enriched number. F. A heat map of relative expression of several CBX7-associated cell cycle genes in TCGA glioblastoma tissues sorted by level of CBX7 expression (r < -0.5). G. MiR-18a regulates Cyclin A2 and CDK2 expression via restoring miR-18a-inhibited CBX7 activation.

a glioblastoma patient. CCK-8 and colony formation assays were performed after transfecting cells with an oligonucleotide inhibitor of miR-18a. We detected significant inhibitory effects on the viabilities of U87 and PG1 cells compared with the controls (**Figure 2A** and **2B**). Further, when we used EDU cell-image assay to evaluate the effect of miR-18a on proliferation, the results were similar to those acquired using the CCK-8 and colony formation assays. Thus, the EDU-positive rates of U87 and PG1 cells were lower compared with those of the controls (**Figure 2C**). The cell cycle was analyzed using flow cytometry. Knockdown of miR-18a induced G1/S arrest and decreased the percentage of cells in S phase. Together, these data indicate that miR-18a expression was associated with oncogenic effects on glioblastoma cells (**Figure 2D**).

CBX7 mRNA is a direct target of miR-18a

To identify the mechanism of the oncogenic effects of miR-18a in glioblastoma cells, we used the bioinformatics analytical tools miRNAWalk 2.0 and TargetScan to identify potential targets of miR-18a. The sequence of the 3'-UTR of *CBX7* mRNA matched the seed sequence of miR-18a. To test the functional significance of this finding, the 3'-UTR sequences containing putative binding sites of the WT or Mut for the seed matching sites were introduced into a luciferase report vector (**Figure 3A**) and each was cotransfected into U87 and PG1 cells with the miR-18a mimic or miR-scramble. Overexpression of miR-18a did not affect the luciferase activities of the CBX7 3'-UTR Mut reporter but decreased the luciferase activity of the WT reporter (**Figure 3B**). Moreover, immunoblotting analysis indicated that CBX7 expression was down-regulated by the miR-18a mimic (**Figure 3G**).

To further investigate the correlation between miR-18a and CBX7 levels, we measured the expression of CBX7 in glioblastoma specimens and adjacent normal brain tissues acquired from 16 patients. The results presented in **Figure 3C** and Supplementary Figure 1A revealed significantly downregulated levels of CBX7 in GBM specimens compared with those in NBT. We further evaluated the correlation of CBX7 and miR-18a levels in the same GBM tissues. Pearson's correlation analysis revealed that the CBX7 levels in the GBM samples inversely correlated with those of miR-18a (Pearson's $r = -0.6264$, $P = 0.0094$). IHC analysis of CBX7 expression was conducted using two representative tissues, including NBT and GBM. CBX7 was mainly detected in nuclei within NBT and was infrequently expressed in GBM tissues (**Figure 3D**).

CBX7-associated genes are mainly involved in the regulation of cell cycle

When we queried three the glioma databases TCGA, CGGA, and GSE4290, we discovered that the transcriptional level of *CBX7* is decreased together with the elevation of glioma grade (Supplementary Figure 1B). Pearson correlation analysis was implemented using MEV software to identify target genes that were negatively associated with *CBX7* expression. We extracted 502 down-regulated genes from the three databases and analyzed them using the DAVID Web tool (http://david.abcc.ncifcrf.gov/home.jsp) for Gene Oncology (GO) and KEGG Pathway enrichment analyses (**Figure 3E**). The down-regulated genes were mainly enriched in the terms positive regulation of cell proliferation, cell cycle and others in the top 5 GO and KEGG Pathway terms of CBX7-acossiated genes. Further, when we conducted coexpression analysis of down-regulated genes in the three databases, we found that the expression of 12 cell cycle-related genes negatively correlated with that CBX7 ($r < -0.5$) (**Figure 3F** and Supplementary Figure 1C). IHC analysis revealed that the regulation of CBX7 by miR-18a was accompanied by alterations of the levels of cyclin A2 and CDK2 in U87 and PG1 cells (**Figure 3G**).

Reintroduction of CBX7 attenuates the effect of miR-18a on the malignant phenotype of glioblastoma cells

To assess the effect of CBX7 on the effects of miR-18a on the malignant phenotype of glioblastoma cells, we cotransfected U87 and PG1 cells with human *CBX7* plasmids and miR-18a mimics. As indicated in **Figure 4A-D**, the increase in proliferation and the distribution of cell cycle induced by miR-18a were inhibited by CBX7 overexpression. Moreover, as shown above, upregulated CBX7 expression alone can significantly inhibit proliferation and promote G1/S cell cycle arrest in U87 and PG1 cells. Further, abnormal CBX7 expression effectively

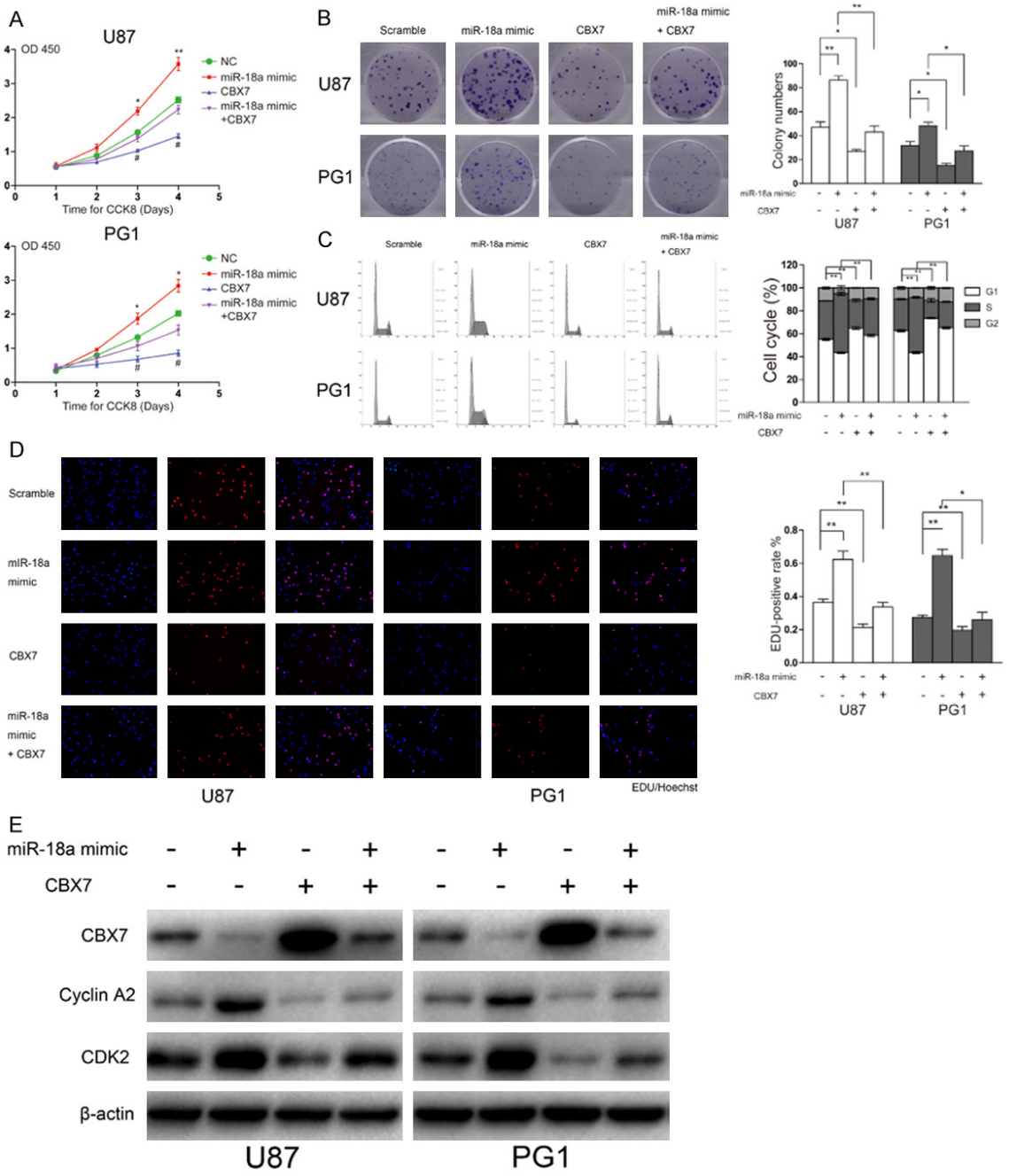

Figure 4. CBX7 reintroduction reverses the promotional effect of miR-18a. A, B. Cell proliferation was detected by CCK8 assay and colony formation assay after U87 and PG1 cells co-transfected miR-18a mimics and CBX7 expression plasmid together or separately. C. The cell proliferative potential was evaluated using the EdU assay 48 h after co-transfection. (original magnification, 200 ×). D. The cell cycle distribution of glioblastoma cells was measured using flow cytometry. E. The levels of the CBX7 and downstream Cyclin A2 and CDK2 were detected by immunoblotting analysis in U87 and PG1 cells co-transfected miR-18a mimics and CBX7 expression plasmid together or separately.

reduced the levels of CDK2 and cyclin A2 expression as well as to recover the positively-modulated levels of CDK2 and cyclin A2 by the miR-18a mimic in U87 and PG1 cells (**Figure 4E**). These results suggest that CBX7 is a functional target of miR-18a in glioblastoma cells.

MiR-18a knockdown inhibits tumor growth in vivo

To determine whether the enhancement of the proliferation of glioblastoma cells by miR-18a affected malignant potential in vivo, we em-

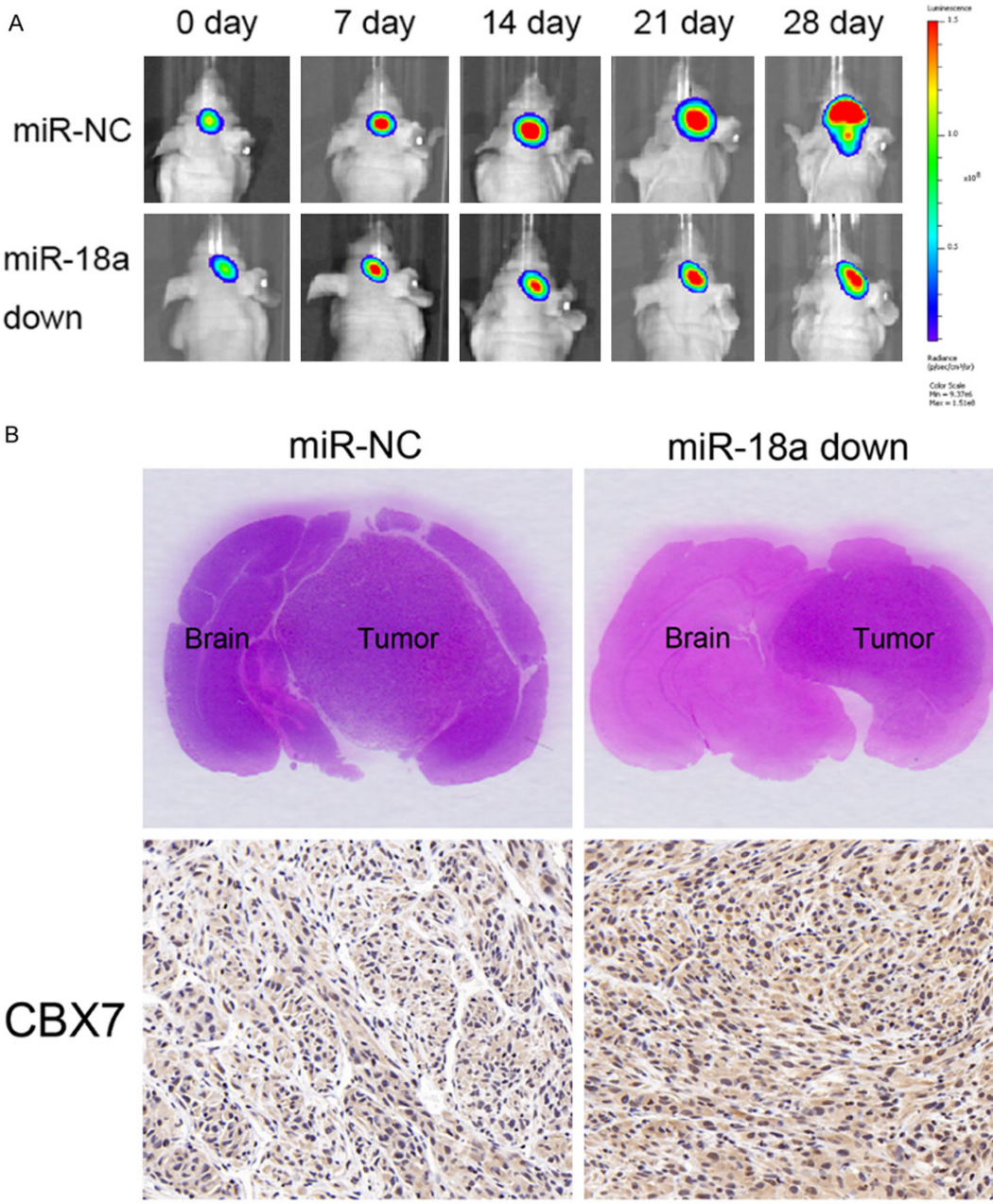
A
0 day
7 day
14 day
21 day
28 day
miR-NC
miR-18a down
B
miR-NC
miR-18a down
Brain
Tumor
Brain
Tumor
CBX7
C
Percent Survival
100
50
0
0
10
20
30
40
miR-NC
miR-18a down
P = 0.011

Figure 5. MiR-18a inhibition suppresses tumor proliferation in vivo. A. U87 cells pretreated with a lentivirus with miR18a-down or miR-NC and a lentivirus containing luciferase were implanted in the brains of nude mice, and tumor formation was assessed by bioluminescence imaging. The bioluminescent images were measured at days 7, 14, 21 and 28 after implantation. B. Tissue slices from representative tumors from two groups of U87 cells were stained with Hematoxylin-eosin-saffron. The images show representative immunohistochemical staining for CBX7. C. Overall survival was determined by Kaplan-Meier survival curves, and a log-rank test was used to assess the statistical significance of the differences.

ployed a U87-xenograft model. Before implantation, U87 glioblastoma cells were coinfected with lentiviruses expressing luciferase with miR-NC or miR18a-down. The intracranial tumor volumes of the miR18a-down groups were significantly reduced compared with those of the miR-NC groups. On days 14, 21, and 28 after implantation, the growth of intracranial tumors was significantly inhibited in association with decreased expression of miR-18a (**Figure 5A**). Moreover, the miR18a-down treatment groups survived significantly longer (**Figure 5C**). At the end of the study, tumor volumes were significantly different between the two groups as revealed by hematoxylin and eosin staining. Further, IHC revealed increased expression of CBX7 in the tumors, which was consistent with the vitro results (**Figure 5B**).

Discussion

MiR-18a, an important member of miR-17-92 family, exerts tumor-specific effects [22-24]. Further, the expression of cell cycle-related proteins is upregulated by overexpression of the miR-17-92 family [25]. MiR-18a is an oncomiR that promotes cell proliferation and facilitates tumor progression [26, 27]. When miR-18a is expressed at abnormally high levels in gastric cancer tissues, it inhibits the expression of interferon regulatory factor 2 to modulate Tumor protein p53 (TP53) expression [28]. MiR-18a promotes the proliferation of esophageal squamous carcinoma cells by increasing cyclin D1 expression [27]. MiR-18a expression is elevated in prostate cancer and promotes tumorigenesis through the suppression of Serine/threonine-protein kinase 4 (STK4) in vitro and in vivo [29]. We show here the upregulated level of miR-18a in glioblastoma tissues. Decreased expression of miR-18a in glioblastoma cells was associated with reduced proliferation ad cell-cycle arrest. Moreover, tumor xenografts in nude mice with reduced levels miR-18a induced by a specific inhibitor slowed tumor growth and prolonged the survival of the engrafted mice.

CBX7 is a member of the polycomb group (PcG) CBX family whose members contain a chromodomain and Polycomb (Pc) box that mediate Pc dimerization and the binding of CBX isoforms to histone H3K27me3 [10, 30]. As a member of the PRC1 family, CBX7 affects the transcription of numerous genes that directly or indirectly influence oncogenesis through recruiting PRC1 to the target chromatin by recognizing H3K-27me3 or not [30]. Accumulating evidence indicates that loss of expression of CBX7 is accompanied by increased aggressiveness of cancers of the colon, thyroid, ovary, and pancreas [15, 16, 31, 32]. CBX7, which is expressed at low levels in GBM, acts as a suppressor of glioma growth [18]. However, the mechanism of the effect of CBX7 on the glioma phenotype is unclear. Here we demonstrate that CBX7 was the direct target of miR-18a, and there was a significant inverse correlation between CBX7 expression and miR-18a levels in GBM tissues. Further, miR-18a inhibit CBX7 expression in vitro and in vivo.

Recently it has been published that CBX7 acts as a tumor suppressor via binding to the promoter of *CCNE1* to recruit HDAC2 to inhibit CCNE1 transcription [17]. We show here that the level of *CBX7* mRNA inversely correlated with malignancy grades in available from three public databases. Further, CBX7-associated genes from the GBM groups of these databases were analyzed using cluster function analysis. These analyses revealed a negative correlation among genes prominently enriched terms associated with the cell cycle. Further, we detected elevated levels of CBX7 that were associated with reduced expression of CDK2 and cyclin A2 in glioblastoma cells. Together, these findings provide strong support for the conclusion that CBX7 is a suppressor of the proliferation of glioma cells.

However, further studies are required to determine the specific mechanism of the elevated expression of miR-18a during the progression of GBM. Further, miR-18a-targeted genes such as *CBX7* require further analysis to determine its functions in gliomas. The specific interac-

tions of CBX7 and cell cycle-related genes involved in tumorigenesis and progress require further study.

In a summary, the present study is the first to our knowledge to reveal that the elevated miR-18a expression of GBM contributed to tumor cell growth in vitro and in vivo, partially through the repression of CBX7 expression. Further, CBX7 negatively regulated the cell cycle in GBM by effectively inhibiting CDK2 and cyclin A2 expression. Our findings therefore provide new insights into the effects of miR-18a and CBX7 during the progression of GBM and that targeting the miR-18a/CBX7 axis may represent a promising therapeutic strategy for managing GBM.

Acknowledgements

We thank Department of Neurosurgery, The First Affiliated Hospital of Nanjing Medical University (Nanjing, China) for its generous help. This work was supported by grants from the Research Special Fund For Public Welfare Industry of Health (201402008), the National Key Research and Development Plan (2016YFC0902500), National Natural Science Foundation of China (81672501, 81472362, 81302185, 81302184), Jiangsu Province's Natural Science Foundation (20131019, 2015-1585), the Program for Advanced Talents within Six Industries of Jiangsu Province (2015-WSN-036, 2016-WSW-013), and the Priority Academic Program Development of Jiangsu Higher Education Institutions (PAPD).

Disclosure of conflict of interest

None.

Address correspondence to: Yongping You, Department of Neurosurgery, The First Affiliated Hospital of Nanjing Medical University, Nanjing 210000, Jiangsu, China. E-mail: taorrren@sina.com

References

[1] Davis ME. Glioblastoma: overview of disease and treatment. Clin J Oncol Nurs 2016; 20: S2-8.

[2] Davis FG and McCarthy BJ. Current epidemiological trends and surveillance issues in brain tumors. Expert Rev Anticancer Ther 2001; 1: 395-401.

[3] He L and Hannon GJ. MicroRNAs: small RNAs with a big role in gene regulation. Nat Rev Genet 2004; 5: 522-531.

[4] Barh D, Malhotra R, Ravi B and Sindhurani P. MicroRNA let-7: an emerging next-generation cancer therapeutic. Curr Oncol 2010; 17: 70-80.

[5] Boyerinas B, Park SM, Hau A, Murmann AE and Peter ME. The role of let-7 in cell differentiation and cancer. Endocr Relat Cancer 2010; 17: F19-36.

[6] Chan JA, Krichevsky AM and Kosik KS. MicroRNA-21 is an antiapoptotic factor in human glioblastoma cells. Cancer Res 2005; 65: 6029-6033.

[7] Si ML, Zhu S, Wu H, Lu Z, Wu F and Mo YY. miR-21-mediated tumor growth. Oncogene 2007; 26: 2799-2803.

[8] Shi Y, Wang Y, Luan W, Wang P, Tao T, Zhang J, Qian J, Liu N and You Y. Long non-coding RNA H19 promotes glioma cell invasion by deriving miR-675. PLoS One 2014; 9: e86295.

[9] Caldas C and Aparicio S. Cell memory and cancer--the story of the trithorax and Polycomb group genes. Cancer Metastasis Rev 1999; 18: 313-329.

[10] Scott CL, Gil J, Hernando E, Teruya-Feldstein J, Narita M, Martinez D, Visakorpi T, Mu D, Cordon-Cardo C, Peters G, Beach D and Lowe SW. Role of the chromobox protein CBX7 in lymphomagenesis. Proc Natl Acad Sci U S A 2007; 104: 5389-5394.

[11] Gil J, Bernard D, Martinez D and Beach D. Polycomb CBX7 has a unifying role in cellular lifespan. Nat Cell Biol 2004; 6: 67-72.

[12] Klauke K, Radulovic V, Broekhuis M, Weersing E, Zwart E, Olthof S, Ritsema M, Bruggeman S, Wu X, Helin K, Bystrykh L and de Haan G. Polycomb Cbx family members mediate the balance between haematopoietic stem cell self-renewal and differentiation. Nat Cell Biol 2013; 15: 353-362.

[13] Kim HY, Park JH, Won HY, Lee JY and Kong G. CBX7 inhibits breast tumorigenicity through DKK-1-mediated suppression of the Wnt/beta-catenin pathway. FASEB J 2015; 29: 300-313.

[14] Hinz S, Kempkensteffen C, Christoph F, Krause H, Schrader M, Schostak M, Miller K and Weikert S. Expression parameters of the polycomb group proteins BMI1, SUZ12, RING1 and CBX7 in urothelial carcinoma of the bladder and their prognostic relevance. Tumour Biol 2008; 29: 323-329.

[15] Karamitopoulou E, Pallante P, Zlobec I, Tornillo L, Carafa V, Schaffner T, Borner M, Diamantis I, Esposito F, Brunner T, Zimmermann A, Federico A, Terracciano L and Fusco A. Loss of the CBX7 protein expression correlates with a more aggressive phenotype in pancreatic cancer. Eur J Cancer 2010; 46: 1438-1444.

[16] Pallante P, Terracciano L, Carafa V, Schneider S, Zlobec I, Lugli A, Bianco M, Ferraro A, Sacchetti S, Troncone G, Fusco A and Tornillo L. The

loss of the CBX7 gene expression represents an adverse prognostic marker for survival of colon carcinoma patients. Eur J Cancer 2010; 46: 2304-2313.

[17] Forzati F, Federico A, Pallante P, Abbate A, Esposito F, Malapelle U, Sepe R, Palma G, Troncone G, Scarfo M, Arra C, Fedele M and Fusco A. CBX7 is a tumor suppressor in mice and humans. J Clin Invest 2012; 122: 612-623.

[18] Nawaz Z, Patil V, Arora A, Hegde AS, Arivazhagan A, Santosh V and Somasundaram K. Cbx7 is epigenetically silenced in glioblastoma and inhibits cell migration by targeting YAP/TAZ-dependent transcription. Sci Rep 2016; 6: 27753.

[19] Shi Z, Chen Q, Li C, Wang L, Qian X, Jiang C, Liu X, Wang X, Li H, Kang C, Jiang T, Liu LZ, You Y, Liu N and Jiang BH. MiR-124 governs glioma growth and angiogenesis and enhances chemosensitivity by targeting R-Ras and N-Ras. Neuro Oncol 2014; 16: 1341-1353.

[20] Zhang R, Luo H, Wang S, Chen W, Chen Z, Wang HW, Chen Y, Yang J, Zhang X, Wu W, Zhang SY, Shen S, Dong Q, Zhang Y, Jiang T, Lu D, Zhao S, You Y, Liu N and Wang H. MicroRNA-377 inhibited proliferation and invasion of human glioblastoma cells by directly targeting specificity protein 1. Neuro Oncol 2014; 16: 1510-1522.

[21] Zhang J, Chen L, Han L, Shi Z, Zhang J, Pu P and Kang C. EZH2 is a negative prognostic factor and exhibits pro-oncogenic activity in glioblastoma. Cancer Lett 2015; 356: 929-936.

[22] Takakura S, Mitsutake N, Nakashima M, Namba H, Saenko VA, Rogounovitch TI, Nakazawa Y, Hayashi T, Ohtsuru A and Yamashita S. Oncogenic role of miR-17-92 cluster in anaplastic thyroid cancer cells. Cancer Sci 2008; 99: 1147-1154.

[23] Ottman R, Levy J, Grizzle WE and Chakrabarti R. The other face of miR-17-92a cluster, exhibiting tumor suppressor effects in prostate cancer. Oncotarget 2016; [Epub ahead of print].

[24] Mouw JK, Yui Y, Damiano L, Bainer RO, Lakins JN, Acerbi I, Ou G, Wijekoon AC, Levental KR, Gilbert PM, Hwang ES, Chen YY, Weaver VM. Tissue mechanics modulate microRNA-dependent PTEN expression to regulate malignant progression. Nat Med 2014; 20: 360-367.

[25] Attar M, Arefian E, Nabiuni M, Adegani FJ, Bakhtiari SH, Karimi Z, Barzegar M and Soleimani M. MicroRNA 17-92 expressed by a transposone-based vector changes expression level of cell-cycle-related genes. Cell Biol Int 2012; 36: 1005-1012.

[26] Luo Z, Dai Y, Zhang L, Jiang C, Li Z, Yang J, McCarthy JB, She X, Zhang W, Ma J, Xiong W, Wu M, Lu J, Li X, Li X, Xiang J and Li G. MiR-18a promotes malignant progression by impairing microRNA biogenesis in nasopharyngeal carcinoma. Carcinogenesis 2013; 34: 415-425.

[27] Zhang W, Lei C, Fan J and Wang J. MiR-18a promotes cell proliferation of esophageal squamous cell carcinoma cells by increasing cylin D1 via regulating PTEN-PI3K-AKT-mTOR signaling axis. Biochem Biophys Res Commun 2016; 477: 144-149.

[28] Chen YJ, Wu H, Zhu JM, Li XD, Luo SW, Dong L, Liu TT and Shen XZ. MicroRNA-18a modulates P53 expression by targeting IRF2 in gastric cancer patients. J Gastroenterol Hepatol 2016; 31: 155-163.

[29] Hsu TI, Hsu CH, Lee KH, Lin JT, Chen CS, Chang KC, Su CY, Hsiao M and Lu PJ. MicroRNA-18a is elevated in prostate cancer and promotes tumorigenesis through suppressing STK4 in vitro and in vivo. Oncogenesis 2014; 3: e99.

[30] Wu JI, Lessard J and Crabtree GR. Understanding the words of chromatin regulation. Cell 2009; 136: 200-206.

[31] Pallante P, Federico A, Berlingieri MT, Bianco M, Ferraro A, Forzati F, Iaccarino A, Russo M, Pierantoni GM, Leone V, Sacchetti S, Troncone G, Santoro M and Fusco A. Loss of the CBX7 gene expression correlates with a highly malignant phenotype in thyroid cancer. Cancer Res 2008; 68: 6770-6778.

[32] Shinjo K, Yamashita Y, Yamamoto E, Akatsuka S, Uno N, Kamiya A, Niimi K, Sakaguchi Y, Nagasaka T, Takahashi T, Shibata K, Kajiyama H, Kikkawa F and Toyokuni S. Expression of chromobox homolog 7 (CBX7) is associated with poor prognosis in ovarian clear cell adenocarcinoma via TRAIL-induced apoptotic pathway regulation. Int J Cancer 2014; 135: 308-318.

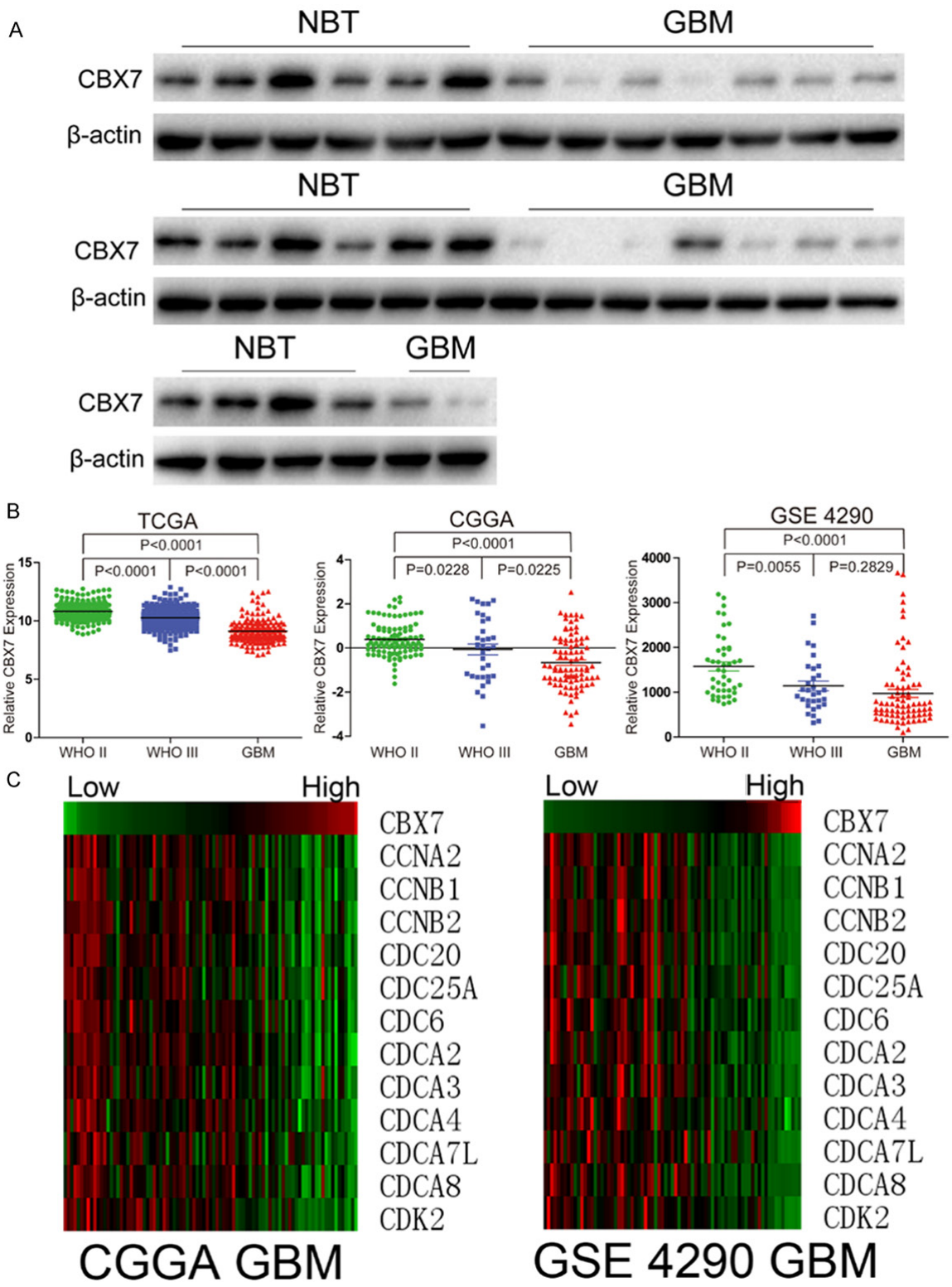

Supplementary Figure 1. A. The expression levels of CBX7 in 16 cases of glioblastoma specimens and adjacent normal brain tissues were determined by immunoblotting, the fold changes were normalized to β-actin. B. Expression of CBX7 negatively correlates with WHO grade in TCGA, CGGA and GSE4290 Public databases. C. A heat map of relative expression of several CBX7-associated cell cycle genes in CGGA and GSE4290 glioblastoma tissues sorted by level of CBX7 expression.